

Chemical Science

Accepted Manuscript



This is an *Accepted Manuscript*, which has been through the Royal Society of Chemistry peer review process and has been accepted for publication.

Accepted Manuscripts are published online shortly after acceptance, before technical editing, formatting and proof reading. Using this free service, authors can make their results available to the community, in citable form, before we publish the edited article. We will replace this *Accepted Manuscript* with the edited and formatted *Advance Article* as soon as it is available.

You can find more information about *Accepted Manuscripts* in the [Information for Authors](#).

Please note that technical editing may introduce minor changes to the text and/or graphics, which may alter content. The journal's standard [Terms & Conditions](#) and the [Ethical guidelines](#) still apply. In no event shall the Royal Society of Chemistry be held responsible for any errors or omissions in this *Accepted Manuscript* or any consequences arising from the use of any information it contains.

EDGE ARTICLE

Spin Crossover Iron(II) Complexes as PARACEST MRI Thermometers

Cite this: DOI: 10.1039/x0xx00000x

Ie-Rang Jeon,^a Jesse G. Park,^a Chad R. Haney,^b T. David Harris^{a,*}

Received 00th January 2012,

Accepted 00th January 2012

DOI: 10.1039/x0xx00000x

www.rsc.org/

We demonstrate the potential utility of spin crossover iron(II) complexes as temperature-responsive paramagnetic chemical exchange saturation transfer (PARACEST) contrast agents in magnetic resonance imaging (MRI) thermometry. This approach is illustrated in the two molecular complexes $[\text{Fe}(\text{3-bpp})_2]^{2+}$ (3-bpp = 2,6-di(pyrazol-3-yl)pyridine) and $[(\text{Me}_2\text{NPY5Me}_2)\text{Fe}(\text{H}_2\text{O})]^{2+}$ ($\text{Me}_2\text{NPY5Me}_2$ = 4-dimethylamino-2,6-bis(1,1-bis(2-pyridyl)ethyl)pyridine). Variable-temperature magnetic susceptibility data collected for aqueous solutions of these complexes reveal that they exhibit spin crossover behaviour in H_2O over the temperature range 20–60 °C. Selective presaturation of pyrazolyl and coordinated water protons in these complexes, respectively, leads to a significant decrease in the NMR signal intensity of bulk water protons through CEST. The corresponding Z-spectra reveal a strong linear temperature dependence of chemical shift of those protons, 0.23(1) ppm/°C and 1.02(1) ppm/°C, respectively, arising from thermal conversion between low-spin $S = 0$ and high-spin $S = 2$ iron(II), representing 23- and 100-fold higher sensitivity than that afforded by conventional proton resonance frequency shift thermometry. Finally, temperature maps generated for an aqueous solution containing $[(\text{Me}_2\text{NPY5Me}_2)\text{Fe}(\text{H}_2\text{O})]^{2+}$ show excellent agreement with independently measured temperatures of the solution.

The ability to noninvasively measure tissue temperature is critical in a number of medical applications, including hyperthermic tumour ablation,¹ treatment of heart arrhythmias,² thermally-activated drug delivery,³ control of gene expression using heat-sensitive promoters,⁴ and potentially the diagnosis of tumours.⁵ Such procedures require precise knowledge of spatial and temporal variation of temperature, as well as accumulated thermal dose, in order to ensure adequate treatment while avoiding damage to surrounding healthy tissue.⁶ As such, MRI is a promising alternative to conventional thermocouples, owing to its noninvasive nature and good temporal and spatial resolution.^{7–9} A number of temperature-dependent properties of tissue water, including T_1 relaxation,¹⁰ diffusion coefficient,¹¹ and proton resonance frequency (PRF),^{12,13} can be monitored in order to image temperature, often in conjunction with temperature-sensitive contrast agents.^{14–17} Currently, PRF shift is the most commonly employed method for imaging temperature, owing largely to its independence on tissue type and linear response to temperature variation. Nevertheless, its application is limited largely due to its low temperature dependence of ca. -0.01 ppm/°C.¹⁴

Recently, the efficacy of lanthanide-based PARACEST agents in MRI thermometry was demonstrated.^{18–22} The NMR spectra of these agents feature paramagnetically shifted proton

resonances, and the corresponding protons exchange with bulk water protons such that selective presaturation of the labile proton spins decreases the intensity of the bulk water MRI signal.^{23,24} Since the lanthanide ion-induced isotropic shift of the exchangeable protons is temperature-dependent,²⁵ these agents are inherently sensitive to temperature. While this approach can lead to significant improvements in sensitivity over PRF thermometry, the sensitivity is still limited to the inherent temperature shift of the protons associated with the electronic configuration of the lanthanide.

Considering that the temperature sensitivity in PARACEST-based MRI thermometry arises from the strong temperature dependence of chemical shift of exchangeable protons, an ideal agent would feature a sharp temperature dependence of a tunable physical parameter that governs chemical shift. Among such parameters, the electronic spin state, S , of the agent is perhaps the most important, as both contact and dipolar shift vary proportionally to $S(S+1)$.²⁵ As such, even small changes in S can lead to dramatic variation in chemical shift. Accordingly, an ideal temperature-responsive PARACEST agent might feature a value of S that changes significantly with temperature. Iron(II) complexes that exhibit thermally-induced electronic spin crossover represent just such a class of molecules.^{26,27} Indeed, in an octahedral coordination environment, an iron(II)

ion exhibiting spin crossover features population of a low-spin, $S = 0$ ground state at low temperatures, whereas increasing temperature will lead to thermal population of a high-spin, $S = 2$ excited state owing to the contribution of entropy differences associated with the spin degrees of freedom. An additional advantage of this approach is that a proton resonance of a spin crossover complex will shift away from the bulk water resonance with increasing temperature, which may be advantageous in monitoring phenomena associated with elevated tissue temperature. Encouragingly, recent work has shown that high-spin iron(II) complexes can be employed as effective PARACEST agents.²⁸ Herein, we demonstrate the potential utility of spin crossover complexes as PARACEST thermometers by examining the magnetic and spectroscopic properties of two iron(II) complexes, $[\text{Fe}(\text{3-bpp})_2]^{2+}$ and $[(\text{Me}_2\text{NPY5Me}_2)\text{Fe}(\text{H}_2\text{O})]^{2+}$, and by carrying out *in vitro* imaging studies on that latter complex.

In selecting candidate molecules for PARACEST thermometry based on spin crossover, three important criteria must be fulfilled: water solubility and stability, spin crossover in aqueous solution over a temperature range that includes 37 °C, and ligand-based protons that can exchange with bulk water. Among molecular species that have been previously reported, the compound $[\text{Fe}(\text{3-bpp})_2](\text{BF}_4)_2 \cdot 3\text{Et}_2\text{O}$ (**1**, see Figure 1) satisfies all three conditions.^{29,30} The cationic complex in **1** features an iron(II) centre that resides in a local distorted octahedral coordination environment, ligated by two neutral 3-bpp ligands. Each of these ligands contains two pyrazolyl groups, with a mean $\text{Fe} \cdots \text{N}(\text{protonated})$ distance of 3.269(3) Å, whose protons can potentially exchange with those of bulk water. In addition, variable-temperature magnetic measurements previously carried out for **1** revealed the presence of spin crossover between an $S = 0$ ground state and $S = 2$ excited state, both in the solid-state³¹ and in solutions of D_2O ,³⁰ with crossover temperatures of $T_{1/2} = 183$ K and 317 K, respectively.

As a second candidate molecule for this study, the compound $[(\text{Me}_2\text{NPY5Me}_2)\text{Fe}(\text{H}_2\text{O})](\text{BF}_4)_2 \cdot \text{H}_2\text{O}$ (**2**, see Figure 1) was synthesized. This compound was targeted largely due to previous observations of solid-state spin crossover in related pentapyridyl iron(II) complexes.³² Reaction of equimolar amounts of $\text{Me}_2\text{NPY5Me}_2$ and $\text{Fe}(\text{BF}_4)_2 \cdot 6\text{H}_2\text{O}$ in a 9:1 mixture of acetone/water under a dinitrogen atmosphere resulted in the formation of a dark brown solution. Subsequent diffusion of diethyl ether vapour into this solution afforded olive-green, block-shaped crystals of $\text{2} \cdot 3\text{H}_2\text{O}$ suitable for single-crystal X-ray analysis. The structure of the cationic complex in $\text{2} \cdot 3\text{H}_2\text{O}$ (see Figure S1), collected at 100 K, consists of an iron(II) centre residing in a local distorted octahedral coordination environment, with five coordination sites occupied by the neutral $\text{Me}_2\text{NPY5Me}_2$ ligand and the sixth site bound by a water molecule. Within this complex, the coordinated water molecule offers two protons that can potentially exchange with those of bulk water. Finally, the average $\text{Fe}-\text{N}$ bond distance of 1.996(2) Å and $\text{Fe}-\text{O}$ distance of 2.007(1) Å suggest a low-spin, $S = 0$ electronic configuration at 100 K.^{32,33}

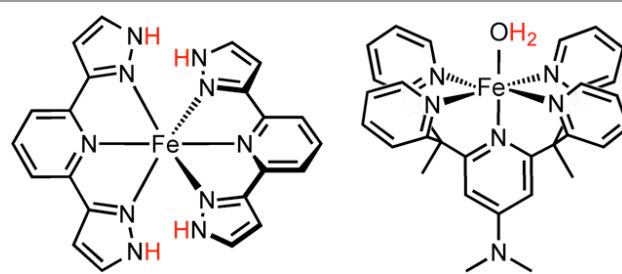


Figure 1. Molecular structures of dications in **1** (left) and **2** (right), with exchangeable protons depicted in red.

In order to probe spin crossover behaviour in **1** and **2**, variable-temperature dc magnetic susceptibility data were collected. As described above, previous measurements carried out for **1** revealed the presence of spin crossover both in the solid-state³¹ and in solutions of D_2O ,³⁰ albeit over different temperature ranges. In order to confirm the presence of similar solution behaviour in H_2O , we examined a 1.0 μM aqueous solution of **1** in the temperature range 293–333 K, in a 9.4 T NMR spectrometer using Evans method.³⁴ Specifically, at 338 K, $\chi_{\text{M}}T = 1.73 \text{ cm}^3\text{Kmol}^{-1}$, considerably lower than the expected value of $3.00 \text{ cm}^3\text{Kmol}^{-1}$ for a fully populated $S = 2$ excited state with $g = 2$. As temperature is lowered, $\chi_{\text{M}}T$ decreases to a minimum value of $0.44 \text{ cm}^3\text{Kmol}^{-1}$ at 293 K, higher than the expected value of $0 \text{ cm}^3\text{Kmol}^{-1}$ for a fully populated $S = 0$ ground state. Overall, the temperature dependence of $\chi_{\text{M}}T$ closely mirrors that previously observed for this complex in D_2O .³⁰

Magnetic data collected for a solid-state sample of **2** at 1 T in the temperature range 2–350 K are shown in Figure S2. At 350 K, $\chi_{\text{M}}T = 0.28 \text{ cm}^3\text{Kmol}^{-1}$, indicative of only minor population of an $S = 2$ excited state. As temperature is lowered, $\chi_{\text{M}}T$ drops precipitously, nearing a value of $0 \text{ cm}^3\text{Kmol}^{-1}$ below 250 K. Fitting the $\chi_{\text{M}}T$ vs T data to an ideal solution model³⁵ gives thermodynamic parameters of $\Delta H = 17.3(6) \text{ kJ mol}^{-1}$ and $\Delta S = 29(1) \text{ J mol}^{-1}$, with an estimated crossover temperature of $T_{1/2} = 597(19) \text{ K}$, consistent with similar iron(II) spin crossover complexes.³⁶ Magnetic data were also collected for a 0.5 μM solution of **2** in H_2O at 9.4 T, analogous to those obtained for compound **1** (see Figure 2). The resulting plot $\chi_{\text{M}}T$ vs T shows a similar profile to that of **1**, decreasing from $2.62 \text{ cm}^3\text{Kmol}^{-1}$ at 338 K to $1.44 \text{ cm}^3\text{Kmol}^{-1}$ at 288 K. Most importantly, the data indicate the presence of spin crossover for an aqueous solution of **2** in this temperature range. Moreover, the temperature-dependent population of spin state for aqueous solutions of **1** and **2** suggests that a strong temperature dependence of the exchangeable proton chemical shifts in these complexes may be present.

In order to confirm the presence and the temperature dependence of PARACEST peaks, variable-temperature NMR spectra were collected for aqueous solutions of **1** (10 mM) and **2** (1.6 mM) by applying a series of presaturation pulses at various frequencies using a 9.4 T NMR spectrometer. The corresponding Z-spectrum at each temperature was generated by plotting the normalized water signal intensity (M_z/M_0 , where

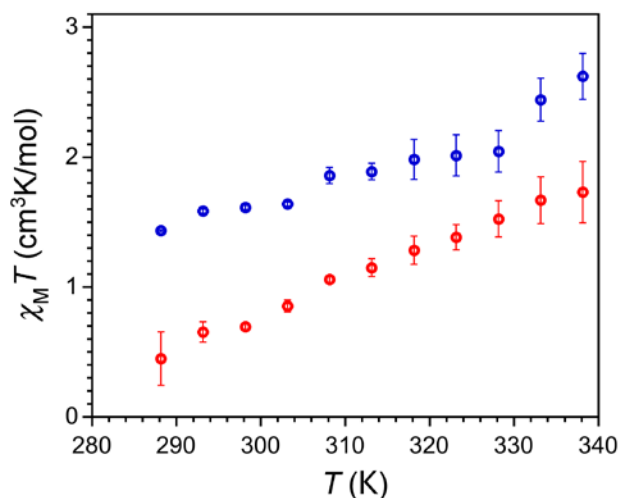


Figure 2. Variable-temperature magnetic susceptibility data for aqueous solutions of **1** (red) and **2** (blue), obtained in a 9.4 T NMR spectrometer using Evans method. Error bars represent standard deviations of the measurements.

M_0 and M_z correspond to the bulk water signal before and after presaturation at a given frequency, respectively) as a function of the presaturation frequency relative to the bulk water frequency, set to 0 ppm (see Figure 3 upper). At 25 °C, the spectrum of **1** exhibits a single CEST peak at 17 ppm vs bulk water with a % CEST effect of 17%. This CEST peak represents the reduction of bulk water intensity that arises from the chemical exchange of bulk water protons with labile pyrazolyl protons. As the temperature is increased, the frequency of the CEST peak shifts away from the bulk water signal, reaching a value at 50 °C of 23 ppm. In addition, this temperature increase is also associated with a gradual increase in peak intensity, which may stem from an increasing proton exchange rate and/or increase in population of the $S = 2$ excited state. The variation in frequency offset of the CEST peak with temperature is nearly linear over the temperature range 25–50 °C, with a linear fit to the data giving a sensitivity of 0.23(1) ppm/°C (see Figure 3 upper, inset). The magnitude of this temperature sensitivity is ca. 23-fold greater than the value of -0.01 ppm/°C afforded by the PRF shift of water. Given the correlation between the temperature dependence of $\chi_M T$ and of the CEST spectrum, we deduce that the temperature dependence of the spectrum arises due to thermal population of the electronic spin states. The increase in frequency offset with temperature further supports this hypothesis, as the isotropic shift of a simple paramagnet invariably decreases with increasing temperature.²⁵

Similar to that obtained for **1**, the spectrum of **2** at 25 °C exhibits a single CEST peak, stemming from proton exchange between coordinated and bulk water, albeit significantly more shifted from bulk water at 30 ppm with a % CEST effect of 15% (see Figure 3 lower). The increased shift relative to **1** may stem in large part to the larger population of a high-spin state in

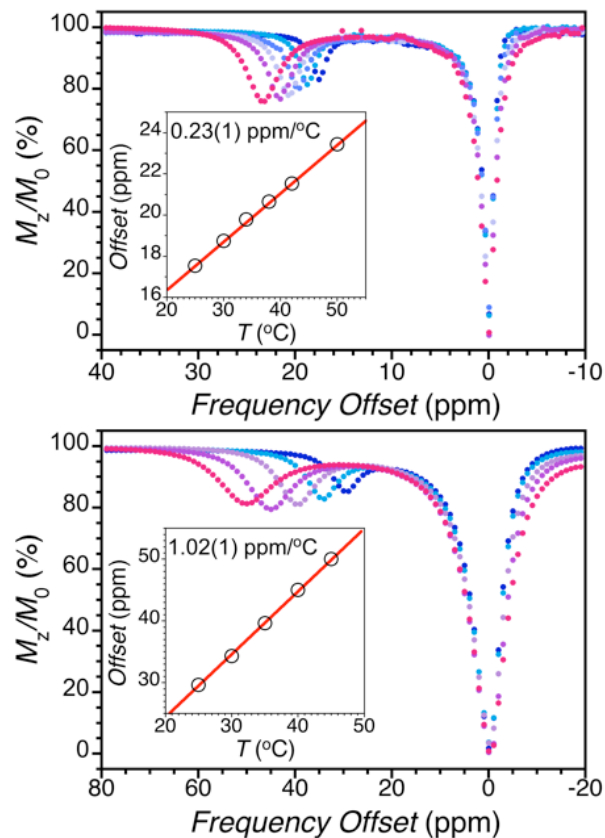


Figure 3. Z-spectra for aqueous solutions containing 10 mM of **1** (upper) and 1.6 mM of **2** (lower), collected at selected temperatures with a 2 s presaturation pulse at 6 μ T and 21 μ T for **1** and **2**, respectively. Insets: temperature dependence of CEST peak offsets.

2 and/or the closer proximity of the exchangeable proton to the paramagnetic centre. As the temperature is increased, the frequency of the CEST peak shifts away from the bulk water signal, reaching a value at 45 °C of 50 ppm. Also analogous to **1**, the variation in frequency offset of the CEST peak with temperature is nearly linear over the temperature range 25–45 °C, however with a much higher temperature sensitivity of 1.02(1) ppm/°C (see Figure 3 lower, inset). This temperature sensitivity is ca. 100-fold greater than the value of -0.01 ppm/°C. Moreover, to our knowledge, this temperature dependence of the CEST peak frequency is the largest yet observed for a PARACEST agent, eclipsing a previously reported Eu³⁺ complex by over 2.5-fold.^{18,19}

Despite the much lower concentration of **2** (1.6 mM) relative to **1** (10 mM), spectra for the two complexes show a comparable CEST effect. The marked enhancement of signal for **2** may largely be attributed to a higher proton exchange rate constant of the coordinated water molecule in **2** compared to the pyrazolyl groups in **1**. Indeed, the rate constant for proton exchange at 25 °C can be estimated as $k_{ex} = 1247(51)$ and $2346(43)$ s⁻¹ for **1** and **2**, respectively, as determined by the omega plot method (see Figure S4).³⁷ The obtained exchange

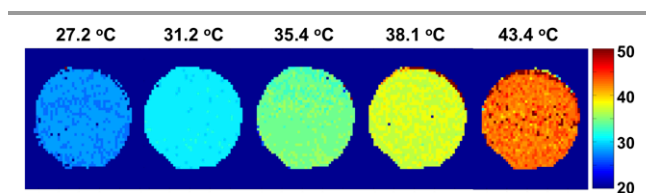


Figure 4. Temperature maps of a phantom containing 1.6 mM of **2** in pH 7 MES buffer solution. Temperatures of the solutions, as obtained independently by a thermocouple, are shown along the top of the figure, and those corresponding to the colour bar (°C) were obtained from the imaging experiment.

rate for **1** is slightly higher than those previously observed for protons of pendant amide substituents in transition metal complexes but significantly lower than one observed for pyrazolyl protons in a cobalt(II) complex.^{28,38} The exchange rate for **2** is comparable to those estimated for protons of water molecules coordinated to Eu³⁺ ions.³⁷ This difference in exchange rate is also evident from the difference in presaturation powers of 6 and 21 μ T employed for **1** and **2**, respectively, as the CEST effect is optimized when the frequency of presaturation power is equal to the exchange rate ($k_{\text{ex}} = 2\pi B_1$).³⁹

Finally, following the observation of strong temperature dependence in the PARACEST spectra of **2**, the possibility of temperature mapping was evaluated by imaging experiments. CEST images were collected for a phantom containing 1.5 mM of compound **2** in pH 7 2-(*N*-morpholino)ethanesulfonic acid (MES) buffer at selected temperatures using a 9.4 T animal MRI scanner (see Figure 4). A series of CEST images over a range of frequencies was acquired at each temperature. Following a previously reported method, the images were analyzed pixel-by-pixel (0.234 mm \times 0.234 mm) such that the presaturation frequency giving the minimum intensity was converted to a temperature using the linear relationship determined from the NMR Z-spectrum, $\delta_{\text{PPM}} = 1.02T + 3.8$.¹⁸ The resulting temperature information is indicated by the colour bars in Figure 4, showing excellent agreement with temperatures independently measured with a thermocouple during the imaging experiment (see Figure S6).

The foregoing results demonstrate that spin crossover iron(II) complexes can be employed as PARACEST contrast agents in MRI thermometry. Two molecular complexes, [Fe(3-bpp)₂]²⁺ and [(Me₂NPY5Me₂)Fe(H₂O)]²⁺, are examined to illustrate this approach. Variable-temperature magnetic susceptibility data obtained for aqueous solutions of these complexes reveal that they exhibit spin crossover behaviour in H₂O over the temperature range 20–60 °C. In line with this observation, variable-temperature Z-spectra reveal a strong linear dependence of chemical shift of those protons, 0.23(1) ppm/°C and 1.02(1) ppm/°C, respectively, representing 23- and 100-fold increases in sensitivity over conventional PRF thermometry. Finally, temperature maps generated for a pH 7 MES solution containing [(Me₂NPY5Me₂)Fe(H₂O)]²⁺ show excellent agreement with independently measured temperatures

of the solution. Efforts are underway to synthesize related complexes with higher stability under physiological conditions, as compound **2** is not robust in oxygenated aqueous solution (see Figure S7), and additionally to incorporate exchangeable protons with resonances that are more highly shifted from bulk water.

Acknowledgements

This research was funded by Northwestern University, the International Institute for Nanotechnology (IIN), and the Chemistry of Life Processes (CLP) Institute through a Chairman's Innovation Award. We thank Ms. A. I. Gaudette, Dr. Y. Zhang, and Dr. W. Morris for experimental assistance, Prof. E. A. Weiss for use of her UV/Visible spectrometer, and Prof. C. A. Mirkin for use of his thermogravimetric analyzer.

Notes and references

^a Department of Chemistry, Northwestern University, 2145 Sheridan Road, Evanston IL 60208-3113

^b Center for Advanced Molecular Imaging, Northwestern University, 2170 Campus Drive, Evanston IL 60208-3113

† Electronic Supplementary Information (ESI) available: Experimental details, crystallographic data for **2**, magnetic data for **2**, spectroscopic data for **1** and **2**, crystallographic information file (CIF) for **2**. See DOI: 10.1039/b000000x/

- (a) M. Ahmed, B. Tasawwar and S. N. Goldberg, *Kidney*, 2013, **8**, 9; (b) Y.-s. Kim, M. J. Park, B. Keserci, K. Nurmailaukas, M. O. Köhler, H. Rhim and H. K. Lim, *Radiology*, 2014, **270**, 589.
- S. Levy, *Arch. Mal. Coeur Vaiss*, 1995, **88**, 1465.
- (a) J. N. Weinstein, R. L. Magin, M. B. Yatvin and D. S. Zaharko, *Science*, 1979, **204**, 188; (b) N. Hijnen, S. Langereis and H. Grüll, *Adv. Drug Deliv. Rev.*, 2014, *in press*.
- R. Deckers, B. Quesson, J. Arsaut, S. Eimer, F. Couillaud and C. T. W. Moonen, *Proc. Nat. Acad. Sci.*, 2009, **106**, 1175.
- R. Jayasundar and V. P. Singh, *Neurol. India*, 2002, **50**, 436.
- H. Rhim, S. N. Goldberg, G.D. Dodd III, L. Solbiati, H. K. Lim, M. Tonolini and O. K. Cho, *Radiographics*, 2001, **21**, S17.
- V. Rieke and K. B. Pauly, *J. Magn. Reson. Imaging*, 2008, **27**, 376.
- B. Quesson, J. A. D. Zwart and C. T. W. Moonen, *J. Magn. Reson. Imaging*, 2000, **12**, 525.
- B. D. Senneville, B. Quesson and C. T. W. Moonen, *Int. J. Hyperthermia*, 2005, **21**, 515.
- D. L. Parker, V. Smith, P. Sheldon, L. E. Crooks and L. Fussell, *Med. Phys.*, 1983, **10**, 321.
- D. Le Bihan, J. Delannoy and R. L. Levin, *Radiology*, 1989, **171**, 853.
- J. C. Hindman, *J. Chem. Phys.* 1966, **44**, 4582.
- Y. Ishihara, A. Calderon, H. Watanabe, K. Okamoto and Y. Suzuki, *Magn. Reson. Med.*, 1995, **34**, 814.
- Lanthanide complexes for spectroscopic imaging: (a) S. Aime, M. Botta, M. Fasano, E. Terreno, P. Kinchesh, L. Calabi and L. Paleari, *MRM*, 1996, **35**, 648; (b) C. S. Zuo, K. R. Metz, M. Y. Sun and A. D. Sherry, *J. Magn. Res.*, 1998, **133**, 53; (c) S. K. Pakin, S. K. Hekmatyar, P. Hopewell, A. Babsky and N. Bansal, *NMR Biomed.*, 2006, **19**, 116; (d) J. R. James, Y. Gao, M. A. Miller, A. Babsky, N.

- Bansal, *Magn. Reson. Med.*, 2009, **62**, 550; (e) D. Coman, H. K. Trubel, F. Hyder, *NMR Biomed.*, 2010, **23**, 277.
- 15 Paramagnetic thermosensitive liposomes: (a) L. H. Lindner, H. M. Reinl, M. Schlemmer, R. Stahl and M. Peller, *Int. J. Hyperthermia*, 2005, **21**, 575; (b) S. Langereis, J. Keupp, L. J. van Velthoven, I. H. C. de Roos, D. Burdinski, J. A. Pikkemaat and H. Gröll, *J. Am. Chem. Soc.*, 2009, **131**, 1380.
- 16 Spin crossover nanoparticles and metallic gadolinium for modification of T_2^* : (a) R. N. Muller, L. Vander Elst and S. Laurent, *J. Am. Chem. Soc.*, 2003, **125**, 8405; (b) F. Settecase, M. S. Sussman and T. P. L. Roberts, *Contrast Media Mol. I.*, 2007, **2**, 50.
- 17 Hyperpolarized xenon: F. Schilling, L. Schröder, K. K. Palaniappan, S. Zapf, D. E. Wemmer and A. Pines, *ChemPhysChem*, 2010, **11**, 3529.
- 18 S. R. Zhang, C. R. Malloy and A. D. Sherry, *J. Am. Chem. Soc.*, 2005, **127**, 17572.
- 19 A. X. Li, F. Wojciechowski, M. Suchy, C. K. Jones, R. H. E. Hudson, R. S. Menon and R. Bartha, *Magn. Reson. Med.*, 2008, **59**, 374.
- 20 E. Terreno, D. Delli Castelli, G. Cravotto, L. Milone and S. Aime, *Invest. Radiol.*, 2004, **39**, 235.
- 21 D. Delli Castelli, E. Terreno and S. Aime, *Angew. Chem. Int. Ed.*, 2011, **50**, 1798.
- 22 N. McVicar, A. X. Li, M. Suchy, R. H. E. Hudson, R. S. Menon and R. Bartha, *Magn. Reson. Med.*, 2013, **70**, 1016.
- 23 S. Viswanathan, Z. Kovacs, K. N. Green, J. Ratnakar and D. A. Sherry, *Chem. Rev.*, 2010, **110**, 2960.
- 24 E. Terreno, D. D. Castelli and S. Aime, *Paramagnetic CEST MRI Contrast Agents, in The Chemistry of Contrast Agents in Medical Magnetic Resonance Imaging*, Second Edition (eds A. Merbach, L. Helm and É. Tóth), John Wiley & Sons, Ltd, Chichester, UK, 2013.
- 25 I. Bertini and C. Luchinat, *NMR of Paramagnetic Molecules in Biological Systems*; The Benjamin/Cummings Publishing Company, Inc.; Menlo Park, CA, 1986.
- 26 *Spin Crossover in Transition Metal Compounds*; P. Gülich and H. A. Goodwin, Eds.; Topics in Current Chemistry, Springer: Berlin, 2004, Vol. 1–3.
- 27 *Spin-Crossover Materials: Properties and Applications*; M. A. Halcrow, Ed.; Wiley-VCH: Weinheim, 2013.
- 28 (a) S. J. Dorazio, P. B. Tsitovich, K. E. Sifers, J. A. Sperry and J. R. Morrow, *J. Am. Chem. Soc.*, 2011, **133**, 14154; (b) S. J. Dorazio and J. R. Morrow, *Inorg. Chem.*, 2012, **51**, 7448; (c) S. J. Dorazio and J. R. Morrow, *Eur. J. Inorg. Chem.*, 2012, 2006; (d) P. B. Tsitovich, J. R. Morrow, *Inorg. Chim. Acta*, 2012, **393**, 3.
- 29 K. H. Sugiyarto, D. C. Craig, A. D. Rae and H. A. Goodwin, *Aust. J. Chem.*, 1994, **47**, 869.
- 30 S. A. Barrett, C. V. Kilner and M. A. Halcrow, *Dalton Trans.*, 2011, **40**, 12021.
- 31 H. A. Goodwin and K. H. Sugiyarto, *Chem. Phys. Lett.*, 1987, **139**, 470.
- 32 D. J. Rudd, C. R. Goldsmith, A. P. Cole, D. P. Stack, K. O. Hodgson and B. Hedman, *Inorg. Chem.*, 2005, **44**, 1221.
- 33 C. R. Goldsmith, R. T. Jonas, A. P. Cole and T. D. P. Stack, *Inorg. Chem.*, 2002, **41**, 4642.
- 34 E. M. Schubert, *J. Chem. Edu.*, 1992, **69**, 61.
- 35 P. Atkins and J. De Paula, *Physical Chemistry, 8th Edition* 2006, Ed. Oxford University Press, Chapter 5.
- 36 H. Toftlund and J. J. McGarvey, *Top. Curr. Chem.*, 2004, **233**, 151.
- 37 W. T. Dixon, J. Ren, A. J. M. Lubag, J. Ratnakar, E. Vinogradov, I. Hancu, R. E. Lenkinski and A. D. Sherry, *Magn. Reson. Med.*, 2010, **63**, 625.
- 38 (a) A. O. Olatunde, S. J. Dorazio, J. A. Sperry and J. R. Morrow, *J. Am. Chem. Soc.*, 2012, **134**, 18503; (b) S. J. Dorazio, A. O. Olatunde, J. A. Sperry and J. R. Morrow, *Chem. Commun.*, 2013, **49**, 10025; (c) P. B. Tsitovich, J. A. Sperry, J. R. Morrow, *Angew. Chem. Int. Ed.*, 2013, **52**, 13997.
- 39 D. E. Woessner, S. Zhang, M. E. Merritt and A. D. Sherry, *Magn. Reson. Med.*, 2005, **53**, 790.